

RESEARCH ARTICLE

Quantifying Heart Rate Variability Using Multiscale Fuzzy Dispersion Entropy

CHAE-MIN KIM AND YOUNG-SEOK CHOI , (Member, IEEE)

Department of Electronics and Communications Engineering, Kwangwoon University, Seoul 01897, South Korea

Corresponding author: Young-Seok Choi (yschoi@kw.ac.kr)

This work was supported in part by the Ministry of Science and ICT (MSIT), South Korea, under the Information Technology Research Center (ITRC) support Program Supervised by the Institute for Information and Communications Technology Planning and Evaluation (IITP) under Grant IITP-2024-RS-2022-00156225; and in part by the Excellent Researcher support Project of Kwangwoon University in 2022.

ABSTRACT Heart rate variability (HRV), which is the variation of inter-beat intervals, exhibits complex characteristics on multiple temporal scales due to the balancing function of the autonomic nervous system. Although there are various nonlinear analysis methods for assessing the complexity of HRV, quantifying HRV over multiple scales is lacking. Here, we present a novel multiscale fuzzy dispersion entropy (MFDE) measure that incorporates quantifying fuzzy dispersion entropy over multiple temporal scales. The proposed MFDE comprises two steps: First, a coarse-graining procedure is carried out for the multiscale decomposition of an inter-beat interval. Second, it conducts FDE computation for each coarse-grained time series. It results in the quantification of complexity, reflecting the long-range correlations inherent in HRV. Using synthetic signals and actual electrocardiogram (ECG), we evaluate the performance of MFDE and compare it to the traditional multiscale entropy methods. The results using synthetic signals show better robustness of MFDE for quantifying complexity with various lengths and predefined parameters. The results using ECGs demonstrate that the proposed MFDE leads to more significant discrimination of HRVs of different cardiovascular states regarding p -values from the Mann-Whitney U test. The capability of MFDE can provide a prospective tool for real-time and practical computer-aided diagnosis using HRV analysis.


INDEX TERMS Heart rate variability, RR intervals, complexity, multiscale fuzzy dispersion entropy.

I. INTRODUCTION

Electrocardiogram (ECG) is a medical diagnostic tool that measures and records the electrical activity of the heart [1], [2], [3]. Heart rate variability (HRV), which is the variation of inter-beat intervals between consecutive heartbeats, namely RR intervals, reflects the mechanism that is controlled by the autonomic nervous system (ANS) [4]. Because the fluctuation of heartbeats is controlled by dynamic ANS, RR intervals vary depending on the conditions of ANS [5], [6]. For example, healthy people have higher HRV levels with autonomic health mechanisms, while patients have lower HRV levels because of the insufficient adaption of the ANS [7]. It is known that the physiological mechanisms of healthy

people are more complex than patients with ill-conditioned cardiovascular systems. Thus, the complexity of patients is reduced [8], [9], [10]. However, differentiating the HRVs of patients remains challenging since the HRV level depends on the type of disease. For instance, patients with atrial fibrillation (AF) indicate high HRVs [11], while ones with congestive heart failure (CHF) show low HRVs [12].

Recently, various nonlinear analysis methods, especially entropy measurements, have been widely used in assessing HRVs. Entropy is a quantitative measure of the degree of irregularity of a time series, which has been widely used in various physiological signal analyses, such as electroencephalogram (EEG), electrocardiogram (ECG), and so on [13], [14], [15], [16]. Sample entropy (SE), the negative logarithm of the conditional probability, has gained a lot of attention in analyzing various physiological signals [17].

The associate editor coordinating the review of this manuscript and approving it for publication was Hamed Azami .

However, SE has the shortcoming of having undefined or unreliable values for short signals. As an alternative tool for SE, fuzzy entropy (FE), which uses various fuzzy membership functions to mitigate the threshold effect, has been developed [18]. However, FE is computationally expensive and still sensitive to the length of a time series. To address the issues of SE and FE, dispersion entropy (DE) has been presented [19]. The DE method, which is a technique that considers the dispersion pattern itself, not only provides reliable entropy values for short signals but also has low computational complexity. Recently, fuzzy dispersion entropy (FDE) has been introduced to address the sensitivity for noise of DE by utilizing fuzzy membership functions [20].

Although entropy is a powerful tool for quantifying the randomness of a time series, there are limitations in quantifying the inherent complexity of a physiological time series, which reveals structures with long-range correlations on multiple spatial and temporal scales [9], [21]. In the physiological complexity context, complex fluctuations of a healthy system are similar to 1/f noise that contains long-range correlations, and 1/f decay produces a fractal structure [22]. Compared to the 1/f noise, the white Gaussian noise (WGN), which is completely disordered and more irregular, has a lower complex structure. However, a WGN is assigned to a higher value than 1/f noise on a single scale by conventional entropy algorithms. It suggests the inappropriate entropy for adaptation in quantifying the complexity of biological signals.

To solve the mismatching between complexity and entropy, Costa et al. [9], [21] have proposed the multiscale SE (MSE). A coarse-graining procedure is used to utilize multiple time series with distinct time scales, followed by the computation of SE on each coarse-grained time series. However, the use of the coarse-grained procedure results in an insufficient length of time series for evaluating SE, leading to undefined and inaccurate entropy values. Unreliable entropy values arising with shortened time series are mainly caused by the existence of the threshold parameter of SE. In order to overcome the sensitivity for predefined parameters of the MSE, several multiscale based entropy methods have been introduced [23], [24], [25], [26], [27]. Among them, the multiscale dispersion entropy (MDE) gained popularity due to its ability in biomedical applications [28]. However, previous multiscale based entropy methods possess inherent shortcomings of original single scale based entropy methods where the complexity quantification on multiscale is still unreliable for short physiological signals and easily influenced by predetermined parameters.

To address the above issues, here, a novel multiscale fuzzy dispersion entropy (MFDE), which quantifies the FDE entropy over multiple temporal scales for reflecting dynamic complexity, is presented. The proposed MFDE consists of a multiscale decomposition of a time series by a coarse-graining procedure and quantification of complexity over multiple time scales using FDE computation. To the best of the authors' knowledge, the use of multiscale based

computation of FDE has not been used for biological signals yet. Although FDE is effective for quantifying the uncertainty of time series, it may fail to capture the complexity of physiological signals over multiple temporal scales. By inheriting the advantage of FDE and multiscale based entropy, the MFDE method results in enhanced quantification of complexity with better robustness than conventional multiscale based entropy methods. Throughout the experiments using synthetic signals, i.e., WGN and 1/f noise, the results demonstrate that MFDE is more capable of reflecting complexities of WGN and 1/f noise for various conditions of lengths and predefined parameters. Moreover, using real ECG signals of distinct physiological states, i.e., CHF, AF, and healthy subjects, the proposed MFDE achieves better discrimination of HRV between different groups compared to the conventional MSE and MDE, which is validated by p -values from the Mann-Whitney U test [29].

The contribution of the proposed MFDE is summarized as follows:

- 1) The proposed MFDE not only employs reliable computation even for short-term time series but also reflects long-range correlations inherited in physiological systems.
- 2) The proposed MFDE possesses robustness in quantifying complexity on the length of time series and predefined parameters.
- 3) The proposed MFDE is better capable of discriminating complexity in HRV of distinct physiological states, especially for short-term time series.

Given the capability of MFDE, it may play a role in the rapid monitoring and diagnosis of individuals with a high risk of cardiovascular disease such as cardiac arrhythmias.

The remainder of this paper is organized as follows: In Section II, we introduce the conventional entropy methods, followed by the introduction of the proposed MFDE methods. Section III describes synthetic signals and real ECG datasets. In Section IV, the performance of MFDE using synthetic signals and real ECG recordings is demonstrated. Section V concludes this work.

II. MATERIALS AND METHODS

A. DISPERSION ENTROPY

For the univariate time series $\mathbf{x} = \{x_1, x_2, \dots, x_N\}$ with a length of N , dispersion entropy (DE) proceeds in five steps according to [19].

- 1) The univariate time series $\mathbf{x} = \{x_1, x_2, \dots, x_N\}$ is normalized to time series $\mathbf{y} = \{y_1, y_2, \dots, y_N\}$ by the normal cumulative distribution function (NCDF) as in (1). The components of the series \mathbf{y} have real values from 0 to 1. Without using NCDF, there is a problem of bias to few values because of extremely large or small values compared with a median value.

$$y_i = \frac{1}{\sigma\sqrt{2\pi}} \int_{-\infty}^{x_i} e^{-\frac{(t-y)^2}{2\sigma^2}} dt, \quad i = 1, 2, \dots, N \quad (1)$$

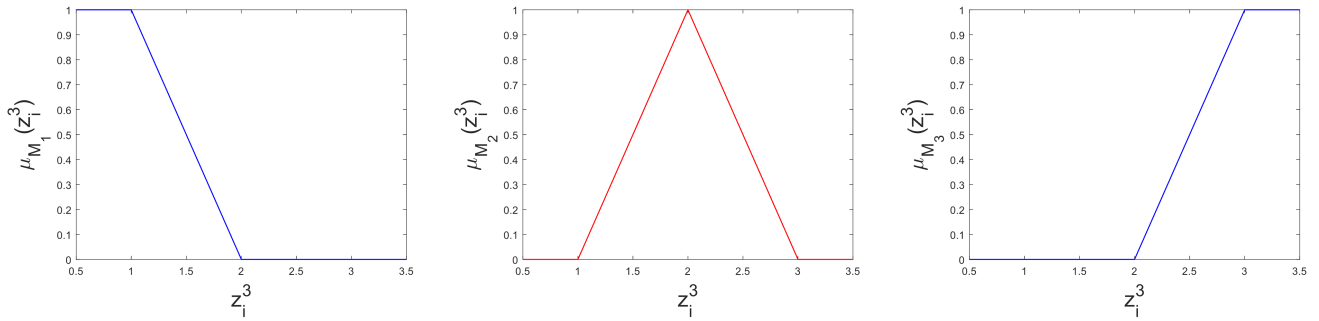


FIGURE 1. Trapezoidal ($k = 1,3$) and triangle membership function ($k = 2$) when the number of classes is $c = 3$.

where γ is the mean and σ is the standard deviation (SD) value of the time series \mathbf{x} .

- 2) The normalized time series $\mathbf{y} = \{y_1, y_2, \dots, y_N\}$ is mapped to the series $\mathbf{z}^c = \{z_1^c, z_2^c, \dots, z_N^c\}$ by the *round* function as follows:

$$z_i^c = \text{round}(c \cdot y_i + 0.5), i = 1, 2, \dots, N \quad (2)$$

where c is the number of classes. z_i^c is assigned to integer classes 1 to c by the *round* function.

- 3) The embedding vector $\mathbf{z}_i^{m,c}$ that has z_i^c as members is created as follows:

$$\mathbf{z}_i^{m,c} = \{z_i^c, z_{i+d}^c, \dots, z_{i+(m-1)d}^c\}, \quad i = 1, 2, \dots, N - (m - 1) d \quad (3)$$

where m is the embedding dimension, c is the number of classes and d is the time delay. $\mathbf{z}_i^{m,c}$ is mapped to a dispersion pattern $\pi_{v_0 v_1 \dots v_{m-1}}$. Each member of $\mathbf{z}_i^{m,c}$, $z_i^c, z_{i+d}^c, \dots, z_{i+(m-1)d}^c$, corresponds to the classes v_0, v_1, \dots, v_{m-1} , respectively. Because the dispersion pattern has m classes with values from 1 to c , the number of possible dispersion patterns is c^m .

- 4) The relative frequency of dispersion patterns is calculated as follows (4), as shown at the bottom of the next page, where the numerator of $p(\pi_{v_0 v_1 \dots v_{m-1}})$ represents the number of $\mathbf{z}_i^{m,c}$ with the dispersion pattern $\pi_{v_0 v_1 \dots v_{m-1}}$.
- 5) Finally, $DE(\mathbf{x}, m, c, d)$ is calculated using the Shannon entropy [30] as follows:

$$DE(\mathbf{x}, m, c, d) = - \sum_{\pi=1}^{c^m} p(\pi_{v_0 v_1 \dots v_{m-1}}) \ln p(\pi_{v_0 v_1 \dots v_{m-1}}) \quad (5)$$

where \mathbf{x} is the original time series, m is the embedding dimension, c is the number of classes, and d is the time delay.

B. FUZZY DISPERSION ENTROPY

For the univariate time series $\mathbf{x} = \{x_1, x_2, \dots, x_N\}$ with a length of N , FDE proceeds in six steps according to [17].

- 1) The univariate time series $\mathbf{x} = \{x_1, x_2, \dots, x_N\}$ is normalized to the time series $\mathbf{y} = \{y_1, y_2, \dots, y_N\}$ by NCDF. The NCDF function is the same as (1).

- 2) In DE, a *round* function is included for mapping $\mathbf{y} = \{y_1, y_2, \dots, y_N\}$ to $\mathbf{z}^c = \{z_1^c, z_2^c, \dots, z_N^c\}$. Due to the existence of the *round* function, which maps to a single class only, DE is sensitive to the parameters and signal lengths [20]. Therefore, FDE eliminates the *round* function of DE as follows:

$$z_i^c = c \cdot y_i + 0.5, \quad i = 1, 2, \dots, N \quad (6)$$

where c is the number of classes

- 3) In a way that reflects all classes, fuzzy functions are used instead of a *round* function. The fuzzy membership function M_k is allocated to each class k . Then, the degree of membership $\mu_{M_k}(z_i^c)$ is measured for each class k , satisfying the following

$$\sum_{k=1}^c \mu_{M_k}(z_i^c) = 1 \quad (7)$$

$$\begin{cases} \mu_{M_k}(z_i^c) = 1 & \text{if } 0.5 \leq z_i^c \leq 1 \\ \mu_{M_k}(z_i^c) + \mu_{M_{k+1}}(z_i^c) = 1, k = \lfloor z_i^c \rfloor & \text{if } 1 \leq z_i^c \leq c \\ \mu_{M_k}(z_i^c) = 1 & \text{if } c \leq z_i^c \leq c + 0.5 \end{cases} \quad (8)$$

If the class k is 1 or c , M_k is the trapezoidal membership function. For the class k between 1 and c , M_k is the triangle membership function. The degree of membership $\mu_{M_k}(z_i^c)$ for each class k is as follows:

$$\mu_{M_1}(\alpha) = \begin{cases} 1 & \alpha < 1 \\ 2 - \alpha & 1 < \alpha < 2 \\ 0 & 2 < \alpha \end{cases} \quad (9)$$

$$\mu_{M_k}(\alpha) = \begin{cases} 0 & \alpha < k - 1 \\ \alpha - k + 1 & k - 1 \leq \alpha \leq k \\ k + 1 - \alpha & k \leq \alpha \leq k + 1 \\ 0 & k + 1 < \alpha \end{cases}, \quad 1 < k < c \quad (10)$$

$$\mu_{M_c}(\alpha) = \begin{cases} 0 & \alpha < c - 1 \\ \alpha - c + 1 & c - 1 \leq \alpha \leq c \\ 1 & c < \alpha \end{cases} \quad (11)$$

Fig. 1 shows the example of fuzzy functions when the number of classes is $c = 3$.

- 4) Embedding vector $\mathbf{z}_i^{m,c}$ that has z_i^c as members are generated identically to (3) in DE. The degree of membership $\mu_{\pi_{v_0 v_1 \dots v_{m-1}}}(\mathbf{z}_i^{m,c})$ for the dispersion pattern $\pi_{v_0 v_1 \dots v_{m-1}}$ is defined as follows:

$$\mu_{\pi_{v_0 v_1 \dots v_{m-1}}}(\mathbf{z}_i^{m,c}) = \prod_{j=0}^{m-1} \mu_{M_{v_j}}(\mathbf{z}_{i+j-d}^c) \quad (12)$$

- 5) The probability of the dispersion pattern $\pi_{v_0 v_1 \dots v_{m-1}}$ is defined as follows:

$$p(\pi_{v_0 v_1 \dots v_{m-1}}) = \frac{\sum_{i=1}^{N-(m-1)d} \mu_{\pi_{v_0 v_1 \dots v_{m-1}}}(\mathbf{z}_i^{m,c})}{N - (m - 1) d} \quad (13)$$

- 6) Finally, based on the Shannon entropy [30], FDE is calculated for all dispersion patterns.

$$FDE(\mathbf{x}, m, c, d) = - \sum_{\pi=1}^{c^m} p(\pi_{v_0 v_1 \dots v_{m-1}}) \ln p(\pi_{v_0 v_1 \dots v_{m-1}}) \quad (14)$$

where \mathbf{x} is the original time series, m is the embedding dimension, c is the number of classes, and d is the time delay.

C. MULTISCALE FUZZY DISPERSION ENTROPY

To compute FDE at multiple scales, we propose multiscale fuzzy dispersion entropy (MFDE). We utilize a coarse-graining process for decomposing an original time series into a multiscale time series [9]. The coarse-graining process generates new time series as a collection of mean values of time series within non-overlapping windows. For a given the original univariate time series $\mathbf{x} = \{x_1, x_2, \dots, x_N\}$, the coarse-grained time series $\mathbf{u}^s = \{u_1^s, u_2^s, \dots, u_{\lfloor N/s \rfloor}^s\}$ is generated as follows:

$$u_j^s = \frac{1}{s} \sum_{i=(j-1)s+1}^{j \cdot s} x_i, \quad 1 \leq j \leq \lfloor N/s \rfloor \quad (15)$$

where s is the scale factor and non-overlapping window size. If the scale factor s is 1, the \mathbf{u}^s is identical to the original time series. For the coarse-grained time series $\mathbf{u}^s (s > 1)$, the MFDE follows the same steps as the FDE with the exception of NCDF mapping. In MFDE algorithms, each of the mean and SD values remains the same as the first scale across all scales. This means that the average and SD of the original

signal are used for all scales [25]. The normalized MFDE is calculated by dividing MFDE by the maximum value $\ln(c^m)$.

For the given univariate time series $\mathbf{x} = \{1.2, 3.7, 2.2, 5.0, 4.1, 10.3, 2.7, 6.5, 7.3, 1.6\}$ with the length $N=10$, MFDE with parameter $m = 2, c = 3, d = 1, s = 2$ has the following procedure:

First, a coarse-grained time series $\mathbf{u}^2 = \{u_1^2, u_2^2, \dots, u_5^2\}$ is created through coarse-graining process:

$$u_j^2 = \frac{1}{2} \sum_{i=2(j-1)+1}^{2j} x_i, \quad 1 \leq j \leq \lfloor 10/2 \rfloor = 5$$

Second, the coarse-grained time series \mathbf{u}^2 is mapped to the \mathbf{z}^3 . The $\mathbf{u}^2 = \{2.45, 3.6, 7.2, 4.6, 4.45\}$ is normalized to the series $\mathbf{y} = \{0.242, 0.382, 0.830, 0.519, 0.499\}$ by NCDF, and \mathbf{y} is mapped to the series $\mathbf{z}^3 = \{1.227, 1.647, 2.989, 2.058, 1.996\}$ by (6). The embedding vectors $\mathbf{z}_i^{2,3} = \{z_i^3, z_{i+1}^3\}$, in which i is from 1 to 4, are created from the \mathbf{z}^3 .

Third, the degree of membership $\mu_{\pi_{v_0 v_1}}(\mathbf{z}_i^{2,3})$ for the dispersion pattern $\pi_{v_0 v_1}$ is calculated. Because both the classes v_0 and v_1 have values from 1 to 3, the number of possible dispersion patterns is $3^2 = 9$. Therefore, the patterns can be $(\pi_{11}, \pi_{12}, \pi_{13}, \pi_{21}, \pi_{22}, \pi_{23}, \pi_{31}, \pi_{32}, \pi_{33})$.

For each embedding vector $\mathbf{z}_i^{2,3}$ in which i is from 1 to 4, the degree of membership $\mu_{\pi_{v_0 v_1}}(\mathbf{z}_i^{2,3})$ is calculated for allocated dispersion patterns. For instance, the degree of membership of the $\mathbf{z}_2^{2,3} = \{1.647, 2.989\}$ is calculated as below:

$$\begin{aligned} \mu_{\pi_{12}}(\mathbf{z}_2^{2,3}) &= \mu_{M_1}(z_2^3) \cdot \mu_{M_2}(z_3^3) = 0.0037, \\ \mu_{\pi_{13}}(\mathbf{z}_2^{2,3}) &= \mu_{M_1}(z_2^3) \cdot \mu_{M_3}(z_3^3) = 0.3491, \\ \mu_{\pi_{22}}(\mathbf{z}_2^{2,3}) &= \mu_{M_2}(z_2^3) \cdot \mu_{M_2}(z_3^3) = 0.0069, \\ \mu_{\pi_{23}}(\mathbf{z}_2^{2,3}) &= \mu_{M_2}(z_2^3) \cdot \mu_{M_3}(z_3^3) = 0.6403 \end{aligned}$$

where M_1, M_3 is the trapezoidal membership function, and M_2 is the triangle membership function. For all dispersion patterns other than $\pi_{12}, \pi_{13}, \pi_{22}$, and $\pi_{23}, \mu_{\pi_{v_0 v_1}}(\mathbf{z}_2^{2,3})$ is 0.

Here, let's assume that the *round* function is used in DE instead of the degree of membership $\mu_{\pi_{v_0 v_1}}(\cdot)$. Then, $\mathbf{z}_i^{2,3} = \{1.647, 2.989\}$ are mapped to the integer classes 2 and 3, respectively. Although $z_i^3 = 1.647$ is clearly the real number between 1 and 2, the *round* function forces to map to the integer class 2, excluding the class 3. It causes the DE to be sensitive to the length of the time series and the parameters m and c . FDE overcomes the limitations of DE by reflecting the information of all adjacent classes.

Fourth, the probability of the dispersion pattern $\pi_{v_0 v_1}$ is calculated. For instance, the probabilities of the dispersion

$$p(\pi_{v_0 v_1 \dots v_{m-1}}) = \frac{\text{Number} \{i \mid i \leq N - (m - 1) d, \mathbf{z}_i^{m,c} \text{ has type } \pi_{v_0 v_1 \dots v_{m-1}}\}}{N - (m - 1) d} \quad (4)$$

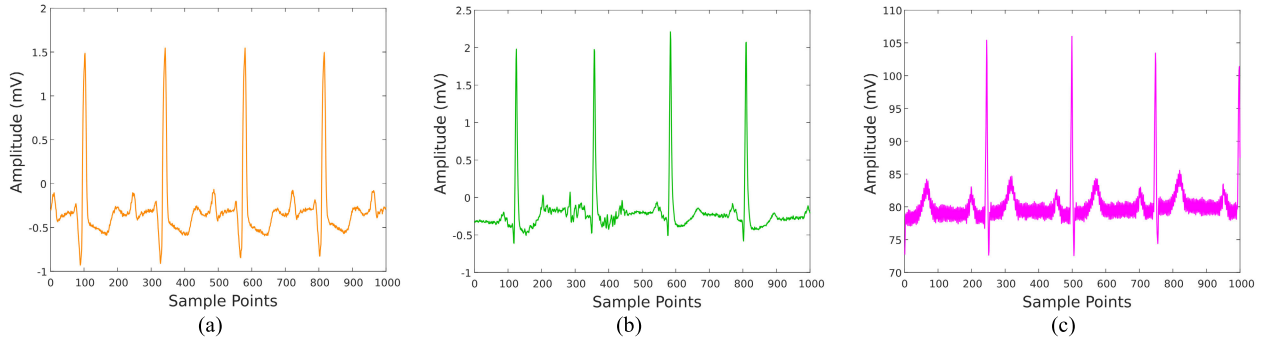


FIGURE 2. ECG data sampled at 250 samples per second: (a) Congestive heart failure (CHF); (b) Atrial fibrillation (AF); (c) Healthy.

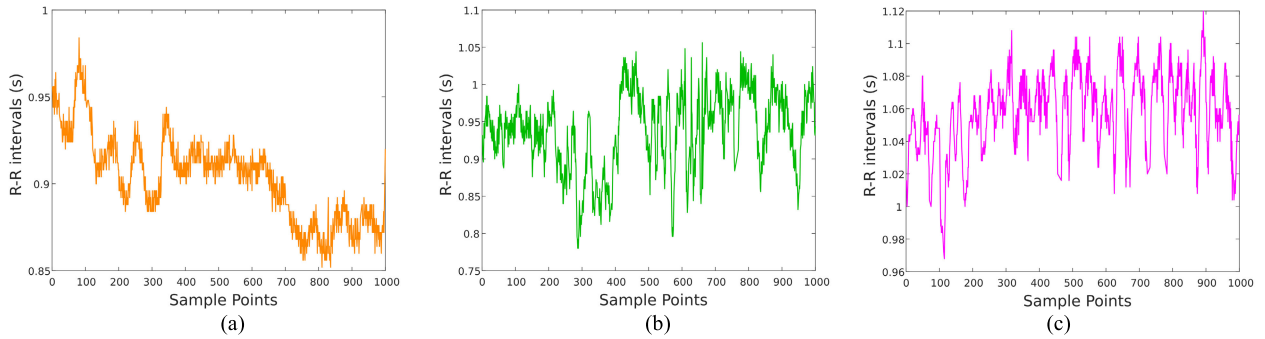


FIGURE 3. RR intervals extracted from ECG data sampled at 250 samples per second: (a) Congestive heart failure (CHF); (b) Atrial fibrillation (AF); (c) Healthy.

patterns π_{12} , π_{13} , π_{22} , and π_{23} are calculated as below:

$$p(\pi_{12}) = \frac{\sum_{j=1}^4 \mu_{\pi_{12}}(\mathbf{z}_j^{2,3})}{4} = \frac{0.5043}{4} = 0.1261,$$

$$p(\pi_{13}) = \frac{\sum_{j=1}^4 \mu_{\pi_{13}}(\mathbf{z}_j^{2,3})}{4} = \frac{0.3491}{4} = 0.0873,$$

$$p(\pi_{22}) = \frac{\sum_{j=1}^4 \mu_{\pi_{22}}(\mathbf{z}_j^{2,3})}{4} = \frac{1.1013}{4} = 0.2753,$$

$$p(\pi_{23}) = \frac{\sum_{j=1}^4 \mu_{\pi_{23}}(\mathbf{z}_j^{2,3})}{4} = \frac{0.6409}{4} = 0.1602$$

Finally, for all possible dispersion patterns, MFDE is calculated as $-\sum_{i=1}^3 \sum_{j=1}^3 p(\pi_{ij}) \ln p(\pi_{ij}) = 1.794$ at the scale factor 2, and the normalized MFDE is $\frac{1.793}{\ln(3^2)} = 0.8164$.

III. EVALUATION SIGNALS

A. SYNTHETIC SIGNALS

Two synthetic signals are used in experiments: white Gaussian noise (WGN) and 1/f noise. WGN has the same energy at all frequencies, which means power spectral density is a constant, and 1/f noise has the characteristics that power spectral density is inversely proportional to frequency [31]. In other words, it means that the energy of 1/f noise contains complex dynamics that vary depending on frequency. Through analysis of multiscale based entropy, it appears that 1/f noise is a more complex structure than WGN [9], [27], [32], [33]. Multiscale entropy values for the synthetic signals,

WGN and 1/f noise, provide important insight with respect to physiological complexity. Besides, 1/f noise, which has a fractal (self-similar) structure, is closely related to the complicated behavior of various physiological signals. Therefore, several multiscale entropy methods still use synthetic signals as performance evaluations for biomedical signals [25], [27], [34].

B. REAL ECG DATASET

Three ECG datasets are publicly available on Physionet [35] and explained precisely as follows. BIDMC CHF database [36] includes ECG recordings from 15 patients (11 men, aged 22 to 71, and 4 women, aged 54 to 63 with severe congestive heart failure NYHA class 3–4). The individual recordings are each about 20 hours in duration, and the sampling frequency is 250Hz. MIT-BIH Atrial Fibrillation database [37] includes 25 ECG recordings of patients with atrial fibrillation (mostly paroxysmal). The individual recordings are each 10 hours in duration, and the sampling frequency is 250 Hz. Fantasia database [38] includes ECG recordings from 40 healthy subjects (twenty young aged 21 to 34 and twenty elderly aged 68 to 85). Each subgroup of subjects includes an equal number of men and women. The individual recordings are each 2 hours in duration, and the sampling frequency is 250 Hz.

The typical ECG signals of the CHF, AF, and healthy subjects are shown in Fig. 2. To analyze HRV, inter-beat intervals, namely RR interval, are extracted from ECGs. RR interval

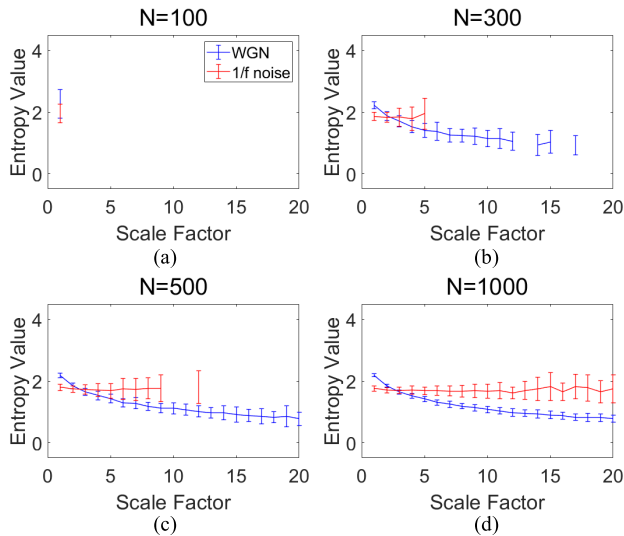


FIGURE 4. MSE of 50 independent WGN and 1/f noise signals; (a) N=100; (b) N=300; (c) N=500; (d) N=1000.

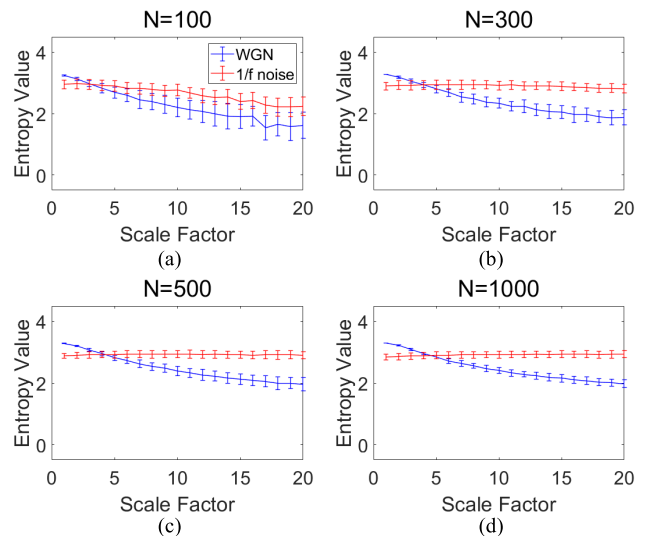


FIGURE 6. MFDE of 50 independent WGN and 1/f noise signals; (a) N=100; (b) N=300; (c) N=500; (d) N=1000.

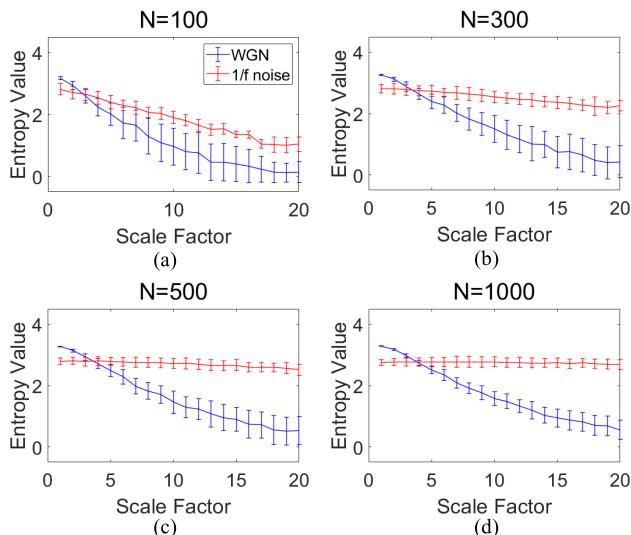


FIGURE 5. MDE of 50 independent WGN and 1/f noise signals; (a) N=100; (b) N=300; (c) N=500; (d) N=1000.

represents the change of time intervals between two consecutive R waves of ECG [39], [40], [41]. Fig. 3 shows the RR intervals of CHF, AF, and healthy subjects, respectively.

IV. EXPERIMENT RESULTS

A. SYNTHETIC SIGNALS

1) DIFFERENT LENGTHS OF SYNTHETIC SIGNALS

To evaluate the performance of the proposed MFDE in terms of the length of synthetic signals, we compare it with the conventional MSE and MDE. All methods use the coarse-graining process with a range of scale factor between 1 and 20. The synthetic signals for the experiment are 50 independent WGNs and 1/f noises with four different lengths (N=100, 300, 500, and 1000). In simulations, MSE, MDE, and MFDE have the following parameters. The parameter of

MSE is $r = 0.2 \times SD$, $m = 2$, $d = 1$, where SD means the standard deviation of the original time series. For MDE and MFDE, $m = 3$, $c = 3$, and $d = 1$ are used.

Fig. 4 shows the MSE of WGN and 1/f noise with length N=100, 300, 500, and 1000. In Fig. 4 (a), MSE values of the noises with N=100 are not defined at all scales except scale 1. In Fig. 4 (b) and (c), there are undefined MSE values with N=300 and N=500 at large scales. It indicates the shortcoming of SE, which is undefined for short signals. Furthermore, the use of a coarse-graining process makes a signal shorter as the scale factor increases, which implies that MSE suffers from analyzing short signals. Fig. 4 (d) shows that all MSE values are defined. Additionally, WGN has higher entropy values for $s < 3$ and lower entropy values for $s > 3$ than 1/f noise. Here, the MSE values of 1/f noise remain constant at all scales, while the MSE values of WGN decrease monotonically. It shows that the 1/f noise has higher complexity than the WGN, which is a consistent result with the complexity analysis of WGN and 1/f noise [27], [34].

Fig. 5 shows the MDE of WGN and 1/f noise with length N=100, 300, 500, and 1000. As shown in Fig. 5, all MDE values are defined for all lengths, unlike MSE. However, in Figs. 5 (a) and (b), the MDE values of the 1/f noise with N=100 and 300 decrease as the scale increases. By comparison, Figs. 5 (c) and (d) indicate that MDE can capture the complexity of WGN and 1/f noises.

Fig. 6 shows the MFDE of WGN and 1/f noise with length N=100, 300, 500, and 1000. As shown in Fig. 6, all MFDE values are defined for all lengths. Notably, as shown in Fig. 6 (a), the MFDE values of WGN and 1/f noise with N=100 are more similar to those with N=1000 compared to the MDE values of WGN and 1/f noise with N=100. Figs. 6 (b)-(d) show that the MFDE values of the 1/f noise with N=300, 500, and 1000 are similar, implying that MFDE is robust to the length of synthetic signals. In addition, the

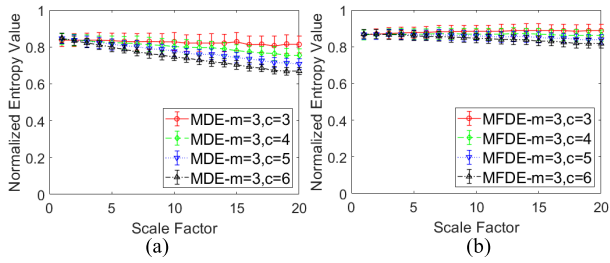


FIGURE 7. Normalized MDE and MFDE of 1/f noise with fixed m and different c ($m = 3, c = 3-6$): (a) Normalized MDE; (b) Normalized MFDE.

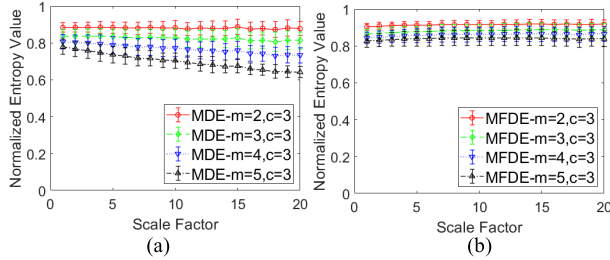


FIGURE 8. Normalized MDE and MFDE of 1/f noise with fixed c and different m ($m = 2-5, c = 3$): (a) Normalized MDE; (b) Normalized MFDE.

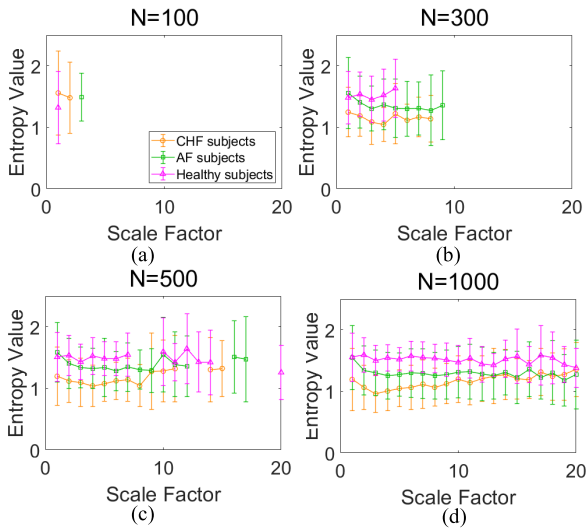


FIGURE 9. MSE of RR intervals extracted from CHF, AF, and Healthy ECG data: (a) $N=100$; (b) $N=300$; (c) $N=500$; (d) $N=1000$.

standard deviations of the MFDE values are lower at most scales than those of MSE and MDE.

Considering the previous works for complexity [9], [10], [42], MFDE significantly enhances the quantification of the complexity of two synthetic signals for various lengths. Especially for short-length cases such as $N=100$ and 300 , the MFDE values of 1/f noise are higher than ones of WGN and remain constant over scales, reflecting its property having long-range correlations. On the other hand, the MSE and MDE values fail to quantify the complexity of two synthetic signals correctly. These observations suggest that MFDE can reflect more accurate complexity regardless of the length of signals and leads to better robustness to the length of signals compared to MSE and MDE.

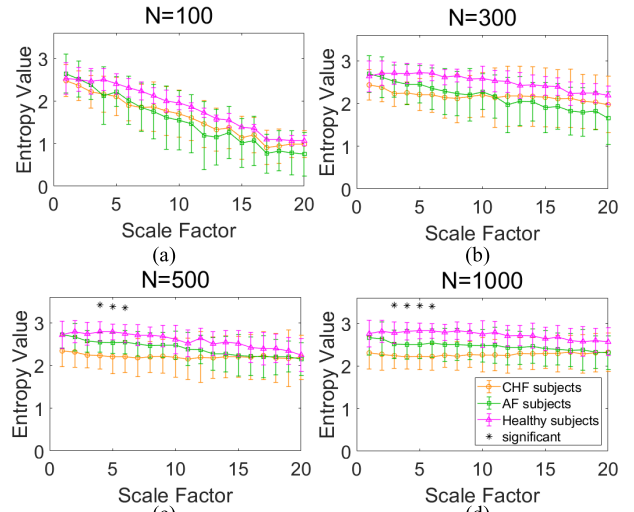


FIGURE 10. MDE of RR intervals extracted from CHF, AF, and Healthy ECG data: (a) $N=100$; (b) $N=300$; (c) $N=500$; (d) $N=1000$.

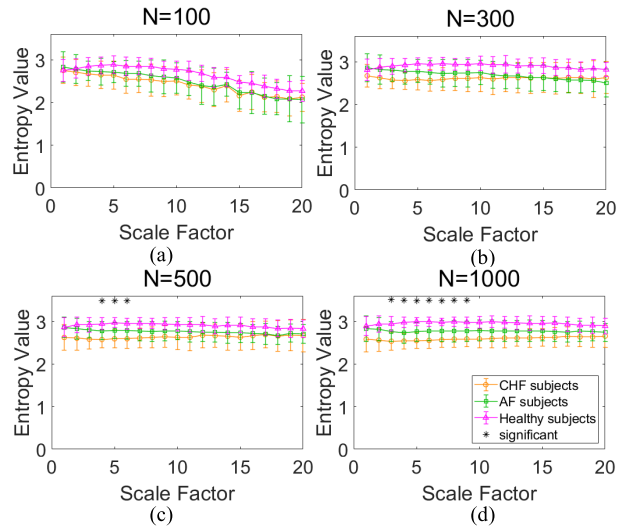


FIGURE 11. MFDE of RR intervals extracted from CHF, AF, and Healthy ECG data: (a) $N=100$; (b) $N=300$; (c) $N=500$; (d) $N=1000$.

2) EFFECT OF PARAMETER ON SYNTHESIZED SIGNALS

To verify the dependency of MDE and the proposed MFDE on predefined parameters, the computation of MDE and MFDE with different values of predefined parameters was carried out.

According to Sections II-A and II-B, MDE and MFDE have common parameters, i.e., the embedding dimension m and the number of class c . The parameters c and m are chosen from 3 to 6 and 2 to 5, respectively. In addition, when one parameter is changing, another parameter is fixed. The synthetic signal 1/f noise with a length of $N=1000$ is used for analyzing the influence of c and m on MDE and MFDE. Normalized MDE and MFDE are used to analyze MDE and MFDE in the same range. All methods use the coarse-graining process for multiscale analysis and the range of scale factor is 1 to 20.

TABLE 1. The MSE p -values between RR intervals of the CHF and AF, AF and Healthy, CHF and Healthy (scale 1- 20). The 'C-A', 'A-H', and 'C-H' are the abbreviations of the comparison of CHF and AF, AF and Healthy, and CHF and Healthy, respectively. 'N/A' denotes 'Not Available'. If a p -value is smaller than 0.05, the value is painted in gray.

scale	N=100			N=300			N=500			N=1000		
	C-A	A-H	C-H	C-A	A-H	C-H	C-A	A-H	C-H	C-A	A-H	C-H
1	N/A	N/A	0.4763	0.1237	0.6295	0.1904	0.0456	0.5053	0.0695	0.0769	0.6961	0.0291
2	N/A	N/A	N/A	0.2064	0.3826	0.0131	0.0769	0.3232	0.0054	0.1354	0.0769	0.0006
3	N/A	N/A	N/A	0.0769	0.2802	0.0108	0.1029	0.3703	0.0258	0.0180	0.1904	0.0002
4	N/A	N/A	N/A	0.0123	0.4483	0.0041	0.0229	0.1611	0.0009	0.0769	0.0508	0.0003
5	N/A	N/A	N/A	0.2234	0.0386	0.0229	0.0508	0.0808	0.0022	0.1029	0.0326	0.0003
6	N/A	N/A	N/A	0.1610	N/A	N/A	0.1904	0.0935	0.0180	0.0849	0.0409	0.0010
7	N/A	N/A	N/A	0.3461	N/A	N/A	0.0769	0.2413	0.0024	0.2234	0.0695	0.0016
8	N/A	N/A	N/A	0.4759	N/A	N/A	0.0291	N/A	N/A	0.2234	0.0229	0.0006
9	N/A	N/A	N/A	N/A	N/A	N/A	0.3232	N/A	N/A	0.3012	0.1354	0.0041
10	N/A	N/A	N/A	N/A	N/A	N/A	0.2232	0.7827	0.0935	0.6625	0.3232	0.0291
11	N/A	N/A	N/A	N/A	N/A	N/A	0.6623	0.7477	0.3118	0.2802	0.1610	0.0028
12	N/A	N/A	N/A	N/A	N/A	N/A	N/A	0.1902	N/A	0.5657	0.2802	0.1129
13	N/A	N/A	N/A	N/A	N/A	N/A	N/A	N/A	N/A	0.8722	0.1478	0.0409
14	N/A	N/A	N/A	N/A	N/A	N/A	N/A	N/A	0.6623	0.8183	0.1477	0.1077
15	N/A	N/A	N/A	N/A	N/A	N/A	N/A	N/A	N/A	0.6295	0.1237	0.0291
16	N/A	N/A	N/A	N/A	N/A	N/A	N/A	N/A	N/A	0.2413	0.7131	0.0695
17	N/A	N/A	N/A	N/A	N/A	N/A	N/A	N/A	N/A	0.6294	0.0365	0.1904
18	N/A	N/A	N/A	N/A	N/A	N/A	N/A	N/A	N/A	0.7652	0.3462	0.1236
19	N/A	N/A	N/A	N/A	N/A	N/A	N/A	N/A	N/A	0.6961	0.0769	0.1752
20	N/A	N/A	N/A	N/A	N/A	N/A	N/A	N/A	N/A	0.6624	0.4213	0.8362

Fig. 7 shows the normalized MDE and MFDE of $1/f$ noise with the different numbers of class c between 3 and 6. As shown in Fig. 7(a), the MDE values of $1/f$ noise tend to decrease for large scales as the number of classes c increases.

On the other hand, Fig. 7(b) demonstrates that the MFDE values of $1/f$ noise remain constant for various values of the number of classes c .

Fig. 8 exhibits the normalized MDE and MFDE of $1/f$ noise in cases where the embedding dimension m varies from 2 to 5. Fig. 8(a) shows that the MDE values of $1/f$ noise decrease for all scales as the embedding dimension m increases. In Fig. 8(b), the MFDE values of $1/f$ noise remain similar for different embedding dimensions.

The results in Figs. 7 and 8 imply that the proposed MFDE can compute complexity robustly in cases of varying pre-defined parameters. On the other hand, the MDE results in inconsistent entropy values if the parameters are changed.

These results are consistent with the fact that the MFDE inherits the strength of FDE less sensitive to the predefined parameters c and m [20]. It might suggest that MFDE is more appropriate for healthcare applications due to its robustness.

B. REAL ECG DATASET

1) VISUAL ANALYSIS OF EXPERIMENT RESULTS

We use RR interval time series extracted from real ECG data which comes from BIDMC CHF, MIT-BIH Atrial

Fibrillation, and Fantasia dataset. The R waves from ECG signals are extracted using the Pan-Tompkins algorithm [43].

Then, the RR interval on the ECG signal represents the time between consecutive R waves, which are the prominent upward spikes seen on an ECG trace. Here, the subjects in each dataset are called CHF, AF, and Healthy, respectively. The complexity of the RR interval is analyzed using MSE, MDE, and MFDE. The parameter of MSE is $r = 0.2 \times SD$, $m = 2$, $c = 3$, and $d = 1$, where SD means the standard deviation of original RR intervals. For MDE and MFDE, $m = 3$, $c = 3$, and $d = 1$ are used. Those parameters are the same as in Section IV-A1. All multiscale entropy methods utilize the coarse-graining process with a range of scale factor between 1 and 20.

To verify the statistical significance, the Mann-Whitney U test was carried out. Here, the significance level of the hypothesis test decision to 0.05, thus if the p -value is less than 0.05, it indicates strong evidence against the null hypothesis, which is the entropy values of two different groups are not discriminated. The asterisks in Figs. 9-11 indicate a significant difference between groups obtained by the Mann-Whitney U test ($p < 0.05$).

Fig. 9 shows the MSE results of RR intervals of the CHF, AF, and Healthy ECG signals with lengths $N=100$, 300, 500, and 1000. In Figs. 9 (a) – (c), the undefined MSE values are happened with $N=100$, 300, and 500 at scale 1, 6, and 8 and above, respectively. It confirms the vulnerability of

TABLE 2. The MDE p -values between RR intervals of the CHF and AF, AF and Healthy, CHF and Healthy (scale 1- 20). The ‘C-A’, ‘A-H’, and ‘C-H’ are the abbreviations of the comparison of CHF and AF, AF and Healthy, and CHF and Healthy, respectively. ‘N/A’ denotes ‘Not Available’. If a p -value is smaller than 0.05, the value is painted in gray.

scale	N=100			N=300			N=500			N=1000		
	C-A	A-H	C-H	C-A	A-H	C-H	C-A	A-H	C-H	C-A	A-H	C-H
1	0.2413	0.3012	0.7652	0.0366	0.6295	0.2064	0.0072	0.9451	0.0123	0.0180	0.5657	0.0026
2	0.2064	0.6625	0.2603	0.1129	0.7652	0.0159	0.0159	0.3232	0.0019	0.0180	0.1611	0.0012
3	0.3232	0.4213	0.0695	0.0180	0.2234	0.0004	0.0072	0.0849	0.0007	0.0291	0.0366	0.0002
4	0.7828	0.0326	0.0258	0.0565	0.1237	0.0003	0.0094	0.0229	0.0002	0.0326	0.0140	0.0001
5	0.5198	0.1536	0.0552	0.1237	0.0849	0.0001	0.0203	0.0054	0.0004	0.0456	0.0082	0.0001
6	0.1470	0.0970	0.0022	0.4213	0.0508	0.0005	0.0159	0.0291	0.0004	0.0159	0.0180	0.0000
7	0.7820	0.0827	0.0217	0.3953	0.1611	0.0005	0.0409	0.0508	0.0022	0.0849	0.0291	0.0001
8	0.7630	0.0682	0.0396	0.6625	0.0180	0.0001	0.0849	0.0159	0.0004	0.0565	0.0159	0.0000
9	0.7084	0.1364	0.1468	0.8362	0.0695	0.0021	0.0769	0.0769	0.0007	0.1478	0.0123	0.0001
10	0.5109	0.0358	0.1978	0.9085	0.0565	0.0094	0.1237	0.3232	0.0123	0.2413	0.0769	0.0016
11	0.7008	0.0777	0.1984	0.7304	0.0432	0.0456	0.2234	0.3462	0.0258	0.1753	0.0366	0.0004
12	0.4623	0.0534	0.1608	0.2412	0.0072	0.0660	0.5053	0.0229	0.0094	0.3012	0.1029	0.0019
13	0.4425	0.0119	0.0631	0.3952	0.0565	0.2802	0.8362	0.0628	0.0326	0.6295	0.0565	0.0014
14	0.6567	0.1736	0.3528	0.0768	0.0077	0.2796	0.9817	0.0456	0.0326	0.3232	0.0695	0.0041
15	0.4660	0.0078	0.0378	0.1473	0.0076	0.3341	0.9085	0.0565	0.0149	0.5657	0.1611	0.0072
16	0.6067	0.1296	0.2736	0.1607	0.0100	0.3818	0.8722	0.1901	0.2063	0.5200	0.0565	0.0054
17	0.2897	0.0078	0.0793	0.0407	0.0256	0.7125	0.7304	0.3231	0.5052	0.9085	0.1237	0.0258
18	0.4212	0.0376	0.1646	0.0759	0.0257	0.9265	0.8361	0.2506	0.3702	0.6961	0.2802	0.0849
19	0.3186	0.1205	0.5491	0.0657	0.0062	0.4192	0.4762	0.2905	0.5351	0.7652	0.0456	0.0628
20	0.1817	0.0583	0.5491	0.1472	0.0201	0.4606	0.5972	0.4622	0.9633	0.7304	0.1129	0.1129

MSE to short-length RR intervals, as previously reported in [24] and [27]. Even though the RR interval length is sufficient, the coarse-grained process prevents the MSE from being computed at large scales. In Fig. 9 (d), although MSE values with N=1000 are defined at all scales, the distinction of distinct groups performs poorly.

Fig. 10 shows the MDE results of RR intervals of the CHF, AF, and Healthy ECG signals with lengths N=100, 300, 500, and 1000. As shown in Figs. 10 (a) – (c), the MDE values are defined at all scales for length N=100, 300, and 500, unlike the MSE. In Figs 10. (c) and (d), in cases of the length is N=500 and 1000, there are significant differences between scales 4 and 6 (Fig. 10 (c), N=500), and between 3 and 6 (Fig. 10 (d), N=1000), respectively. It shows that MDE has better distinction performance than MSE with the same lengths of RR intervals. However, the subjects CHF, AF, and Healthy are not distinguished well at large scales.

Fig. 11 shows the MFDE results of RR intervals of the CHF, AF, and Healthy ECG signals with lengths N=100, 300, 500, and 1000. Figs. 11 (a) – (d) show that MFDE leads to reliable computation at all scales for short and relatively short lengths of signals compared with the existing methods in Figs. 9 and 10. In Figs. 11 (c) and (d), MFDE results with RR intervals with N=500 and 1000 show that there are significant differences between scales 4 and 6 (Fig. 11 (c), N=500), and between 3 and 9 (Fig. 11 (d), N=1000), respectively. Notably, if the length is N=1000, MFDE results in a broader

range of scales in which three groups are statistically distinct compared with MSE and MDE. In addition, the standard deviations of MFDE values with various lengths are lower than those of MDE values over all scales.

Given the results using the synthetic signals in Sec IV-A, although MDE and MFDE appear to have similar discrimination performance, the inaccurate results of MDE for short signals and its susceptibility to parameter variation suggest that MFDE may be a better measure of HRV complexity in the three groups.

2) STATISTICAL ANALYSIS OF EXPERIMENT RESULTS

The Mann-Whitney U test was carried out to verify the discriminating performance of MSE, MDE, and MFDE between two groups. The significance level of the hypothesis test decision to 0.05. The statistical results of pairwise comparison using MSE, MDE, and MFDE are shown in Tables 1-3, respectively. In Tables, if the p -value is less than 0.05, a statistically significant difference is accepted and highlighted as gray in Tables. The notations ‘C-A’, ‘A-H’, and ‘C-H’ denote the abbreviations of the comparison of CHF and AF, AF and Healthy, and CHF and Healthy, respectively.

Table. 1 shows the p -value of the Mann-Whitney U test using MSE of the CHF, AF, and Healthy RR intervals with lengths of N=100, 300, 500, and 1000. In Table. 1, several computations of p -values are unavailable, mainly in cases of N=100, 300, and 500. It means undefined entropy values

TABLE 3. The MFDE *p*-values between RR intervals of the CHF and AF, AF and Healthy, CHF and Healthy (scale 1- 20). The ‘C-A’, ‘A-H’, and ‘C-H’ are the abbreviations of the comparison of CHF and AF, AF and Healthy, and CHF and Healthy, respectively. ‘N/A’ denotes ‘Not Available’. if a *p*-value is smaller than 0.05, the value is painted in gray.

scale	N=100			N=300			N=500			N=1000		
	C-A	A-H	C-H	C-A	A-H	C-H	C-A	A-H	C-H	C-A	A-H	C-H
1	0.4484	0.4213	0.9817	0.0628	0.5351	0.1478	0.0229	0.8722	0.0180	0.0229	0.7304	0.0063
2	0.5657	0.6961	0.5053	0.0628	0.9451	0.0140	0.0409	0.3462	0.0054	0.0159	0.1904	0.0014
3	0.6625	0.1611	0.1129	0.0072	0.4484	0.0010	0.0140	0.1904	0.0009	0.0063	0.0203	0.0002
4	0.4763	0.2064	0.0508	0.0229	0.3703	0.0001	0.0094	0.0366	0.0001	0.0140	0.0123	0.0000
5	0.7304	0.0456	0.0628	0.0508	0.0366	0.0001	0.0159	0.0035	0.0004	0.0082	0.0026	0.0000
6	0.1753	0.0695	0.0140	0.1354	0.0628	0.0001	0.0180	0.0180	0.0003	0.0094	0.0082	0.0000
7	0.2802	0.0935	0.0072	0.3232	0.0508	0.0003	0.0628	0.0180	0.0005	0.0159	0.0140	0.0000
8	0.2234	0.1237	0.0047	0.3232	0.0849	0.0006	0.1611	0.0123	0.0005	0.0366	0.0094	0.0001
9	0.2603	0.2802	0.0063	0.5351	0.0628	0.0003	0.2413	0.0326	0.0012	0.0366	0.0140	0.0001
10	0.4763	0.1129	0.0180	0.3232	0.0565	0.0016	0.1478	0.0456	0.0054	0.0508	0.0326	0.0001
11	0.3703	0.0366	0.0026	0.6295	0.0291	0.0035	0.3953	0.0695	0.0072	0.0628	0.0159	0.0001
12	0.8005	0.0565	0.0409	0.8722	0.0159	0.0041	0.6295	0.0456	0.0140	0.1237	0.0258	0.0002
13	0.6295	0.2064	0.0229	0.9451	0.0565	0.0159	0.6625	0.1354	0.0229	0.0849	0.0366	0.0003
14	0.9817	0.0935	0.1237	0.7652	0.0082	0.0094	0.7304	0.0508	0.0123	0.1129	0.0769	0.0003
15	0.5053	0.0695	0.0094	0.9817	0.0063	0.0159	0.5053	0.0326	0.0063	0.0849	0.0456	0.0003
16	0.8722	0.2064	0.1029	0.4763	0.0159	0.0456	0.7652	0.0508	0.0628	0.2234	0.0203	0.0003
17	0.6625	0.1904	0.0409	0.3462	0.0108	0.0258	0.8005	0.0628	0.1354	0.1904	0.0456	0.0012
18	0.8722	0.0769	0.1029	0.3012	0.0072	0.1354	0.5351	0.0628	0.1478	0.1478	0.0935	0.0014
19	0.6625	0.6625	0.1354	0.3232	0.0047	0.0508	N/A	0.0935	0.1478	0.1611	0.0565	0.0035
20	0.9085	0.4763	0.3462	0.2413	0.0072	0.1904	0.8005	0.1354	0.2802	0.3012	0.0628	0.0072

or *p*-values equal 1.0, where two different samples are not discriminated. It is clear that the shorter the data length is, the more the *p*-values are not available. In addition, the longer the data length is, the more the *p*-values are statistically significant. Especially, the number of significant *p*-values is larger between CHF and Healthy subjects than other comparisons. These results suggest that MSE cannot discriminate the complexity of HRV between different groups for short RR intervals.

Table. 2 shows the *p*-value of the Mann-Whitney U test using MDE of the CHF, AF, and Healthy RR intervals with lengths of N=100, 300, 500, and 1000. In Table. 2, compared to the MSE results, all *p*-values using MDE values are available and there is an increased number of significant *p*-values for all lengths of RR intervals. However, the number of significant *p*-values between CHF and AF is smaller than the comparison of AF and Healthy and CHF and Healthy. In other words, although the discriminative ability of the MDE is superior to that of the MSE, it still suffers from distinguishing between the patient groups CHF and AF.

In Table. 3, the *p*-value of the Mann-Whitney U test utilizing MFDE is displayed for the same comparison. As shown in Table. 3, MFDE leads to significantly more significant pairwise discriminations than MSE, regardless of the length of the RR intervals. In the case of discrimination between AF and Healthy, the discrimination performance of MFDE

is better or comparable to that of MDE in comparison to its results except for N=100. Besides, for all lengths, MFDE performs noticeably well in discriminating between CHF and Healthy. It is noteworthy that MFDE is superior to MDE in terms of discriminating between CHF and AF for N=1000.

It has been known that the classification between CHF or AF disorder from a normal condition is most important [1], [44]. Generally, MFDE has a superior ability to differentiate between cardiovascular patients (CHF, AF) and the healthy than MSE and MDE. However, distinguishing between CHF and AF for short lengths of ECGs remains a challenge.

The proposed method for discriminating abnormal ECGs with short-term ECGs may provide a significant step forward in cardiac health monitoring. Its potential for application in clinical settings and further research could lead to remarkable improvements in cardiovascular disease diagnosis and treatment. Furthermore, integrating this technique into wearable ECG monitoring devices could pave the way for continuous, real-time monitoring of patients at high risk.

V. CONCLUSION

For an improved quantification of the variation of inter-beat intervals, namely HRV, we have proposed a multiscale-based entropy utilizing FDE, named MFDE. The proposed MFDE possesses a stable computation of complexity using time series with short and sufficient lengths compared to

conventional MSE and MDE. In addition, MFDE achieves a more robust quantification of complexity on the predefined parameters. Through experiments using synthetic signals and real ECG signals, the results show that MFDE improves a capability for representing complexity regardless of the length of time series. By applying MFDE for discriminating distinct physiological statuses using RR intervals, it achieves an improvement over widely used entropy measures. While promising, this work has a limitation on a coarse-grained procedure. Future work needs to develop a refined version of multiscale decomposition. Considering the properties of the proposed MFDE, it might play an essential role in utilizing HRV for a variety of applications.

REFERENCES

- [1] G. Valenza, L. Faes, N. Toschi, and R. Barbieri, "Advanced computation in cardiovascular physiology: New challenges and opportunities," *Phil. Trans. Roy. Soc. A, Math., Phys. Eng. Sci.*, vol. 379, no. 2212, Dec. 2021, Art. no. 20200265, doi: [10.1098/rsta.2020.0265](https://doi.org/10.1098/rsta.2020.0265).
- [2] G. Adasuriya and S. Haldar, "Next generation ECG: The impact of artificial intelligence and machine learning," *Current Cardiovascular Risk Rep.*, vol. 17, no. 8, pp. 143–154, Aug. 2023, doi: [10.1007/s12170-023-00723-4](https://doi.org/10.1007/s12170-023-00723-4).
- [3] P. D. Lambiase and E. Maclean, "Review of the national institute for health and care excellence guidelines on the management of atrial and ventricular arrhythmias," *Heart*, vol. 110, no. 5, pp. 313–322, Jul. 2023, doi: [10.1136/heartjnl-2022-322122](https://doi.org/10.1136/heartjnl-2022-322122).
- [4] U. R. Acharya, K. P. Joseph, N. Kannathal, C. M. Lim, and J. S. Suri, "Heart rate variability: A review," *Med. Biol. Eng. Comput.*, vol. 44, no. 12, pp. 1031–1051, Dec. 2006, doi: [10.1007/s11517-006-0119-0](https://doi.org/10.1007/s11517-006-0119-0).
- [5] F. Shaffer and J. P. Ginsberg, "An overview of heart rate variability metrics and norms," *Frontiers Public Health*, vol. 5, p. 258, Sep. 2017. Accessed: Sep. 24, 2023. [Online]. Available: <https://www.frontiersin.org/articles/10.3389/fpubh.2017.00258>
- [6] Y. Yaniv and A. E. Lyashkov, "The fractal-like complexity of heart rate variability beyond neurotransmitters and autonomic receptors: Signaling intrinsic to sinoatrial node pacemaker cells," *Cardiovascular Pharmacol., Open Access*, vol. 2, no. 3, p. 111, 2013.
- [7] L. C. M. Vanderlei, C. M. Pastre, R. A. Hoshi, T. D. de Carvalho, and M. F. de Godoy, "Basic notions of heart rate variability and its clinical applicability," *Braz. J. Cardiovasc. Surg.*, vol. 24, pp. 205–217, Jun. 2009, doi: [10.1590/S0102-76382009000200018](https://doi.org/10.1590/S0102-76382009000200018).
- [8] A. L. Goldberger, C.-K. Peng, and L. A. Lipsitz, "What is physiological complexity and how does it change with aging and disease?" *Neurobiol. Aging*, vol. 23, no. 1, pp. 23–26, Jan. 2002, doi: [10.1016/S0197-4580\(01\)00266-4](https://doi.org/10.1016/S0197-4580(01)00266-4).
- [9] M. Costa, A. L. Goldberger, and C.-K. Peng, "Multiscale entropy analysis of biological signals," *Phys. Rev. E, Stat. Phys. Plasmas Fluids Relat. Interdiscip. Top.*, vol. 71, no. 2, Feb. 2005, Art. no. 2, doi: [10.1103/physreve.71.021906](https://doi.org/10.1103/physreve.71.021906).
- [10] L. E. V. Silva, B. C. T. Cabella, U. P. D. C. Neves, and L. O. M. Junior, "Multiscale entropy-based methods for heart rate variability complexity analysis," *Phys. A, Stat. Mech. Appl.*, vol. 422, pp. 143–152, Mar. 2015, doi: [10.1016/j.physa.2014.12.011](https://doi.org/10.1016/j.physa.2014.12.011).
- [11] A. M. Catai, C. M. Pastre, M. F. D. Godoy, E. D. Silva, A. C. D. M. Takahashi, and L. C. M. Vanderlei, "Heart rate variability: Are you using it properly? Standardisation checklist of procedures," *Brazilian J. Phys. Therapy*, vol. 24, no. 2, pp. 91–102, Mar. 2020, doi: [10.1016/j.bjpt.2019.02.006](https://doi.org/10.1016/j.bjpt.2019.02.006).
- [12] C.-S. Poon and C. K. Merrill, "Decrease of cardiac chaos in congestive heart failure," *Nature*, vol. 389, no. 6650, pp. 492–495, Oct. 1997, doi: [10.1038/39043](https://doi.org/10.1038/39043).
- [13] T. Li and M. Zhou, "ECG classification using wavelet packet entropy and random forests," *Entropy*, vol. 18, no. 8, p. 285, Aug. 2016, doi: [10.3390/e18080285](https://doi.org/10.3390/e18080285).
- [14] A. Asgharzadeh-Bonab, M. C. Amirani, and A. Mehri, "Spectral entropy and deep convolutional neural network for ECG beat classification," *Biocybern. Biomed. Eng.*, vol. 40, no. 2, pp. 691–700, Apr. 2020, doi: [10.1016/j.bbe.2020.02.004](https://doi.org/10.1016/j.bbe.2020.02.004).
- [15] N. Arunkumar, K. R. Kumar, and V. Venkataraman, "Entropy features for focal EEG and non focal EEG," *J. Comput. Sci.*, vol. 27, pp. 440–444, Jul. 2018, doi: [10.1016/j.jocs.2018.02.002](https://doi.org/10.1016/j.jocs.2018.02.002).
- [16] R. Sun, R. Song, and K.-Y. Tong, "Complexity analysis of EMG signals for patients after stroke during robot-aided rehabilitation training using fuzzy approximate entropy," *IEEE Trans. Neural Syst. Rehabil. Eng.*, vol. 22, no. 5, pp. 1013–1019, Sep. 2014, doi: [10.1109/TNSRE.2013.2290017](https://doi.org/10.1109/TNSRE.2013.2290017).
- [17] J. S. Richman and J. R. Moorman, "Physiological time-series analysis using approximate entropy and sample entropy," *Amer. J. Physiol.-Heart Circulatory Physiol.*, vol. 278, no. 6, pp. 2039–2049, Jun. 2000, doi: [10.1152/ajpheart.2000.278.6.h2039](https://doi.org/10.1152/ajpheart.2000.278.6.h2039).
- [18] W. Chen, Z. Wang, H. Xie, and W. Yu, "Characterization of surface EMG signal based on fuzzy entropy," *IEEE Trans. Neural Syst. Rehabil. Eng.*, vol. 15, no. 2, pp. 266–272, Jun. 2007, doi: [10.1109/TNSRE.2007.897025](https://doi.org/10.1109/TNSRE.2007.897025).
- [19] M. Rostaghi and H. Azami, "Dispersion entropy: A measure for time-series analysis," *IEEE Signal Process. Lett.*, vol. 23, no. 5, pp. 610–614, May 2016, doi: [10.1109/LSP.2016.2542881](https://doi.org/10.1109/LSP.2016.2542881).
- [20] M. Rostaghi, M. M. Khatibi, M. R. Ashory, and H. Azami, "Fuzzy dispersion entropy: A nonlinear measure for signal analysis," *IEEE Trans. Fuzzy Syst.*, vol. 30, no. 9, pp. 3785–3796, Sep. 2022, doi: [10.1109/TFUZZ.2021.3128957](https://doi.org/10.1109/TFUZZ.2021.3128957).
- [21] M. Costa, A. L. Goldberger, and C.-K. Peng, "Multiscale entropy analysis of complex physiologic time series," *Phys. Rev. Lett.*, vol. 89, no. 6, Jul. 2002, Art. no. 6, doi: [10.1103/physrevlett.89.068102](https://doi.org/10.1103/physrevlett.89.068102).
- [22] H. Azami and J. Escudero, "Refined composite multivariate generalized multiscale fuzzy entropy: A tool for complexity analysis of multichannel signals," *Phys. A, Stat. Mech. Appl.*, vol. 465, pp. 261–276, Jan. 2017, doi: [10.1016/j.physa.2016.07.077](https://doi.org/10.1016/j.physa.2016.07.077).
- [23] D.-Y. Lee and Y.-S. Choi, "Multiscale distribution entropy analysis of short-term heart rate variability," *Entropy*, vol. 20, no. 12, p. 952, Dec. 2018, Art. no. 12, doi: [10.3390/e20120952](https://doi.org/10.3390/e20120952).
- [24] D.-Y. Lee and Y.-S. Choi, "Multiscale distribution entropy analysis of heart rate variability using differential inter-beat intervals," *IEEE Access*, vol. 8, pp. 48761–48773, 2020, doi: [10.1109/ACCESS.2020.2978930](https://doi.org/10.1109/ACCESS.2020.2978930).
- [25] H. Azami, S. E. Arnold, S. Sanei, Z. Chang, G. Sapiro, J. Escudero, and A. S. Gupta, "Multiscale fluctuation-based dispersion entropy and its applications to neurological diseases," *IEEE Access*, vol. 7, pp. 68718–68733, 2019, doi: [10.1109/ACCESS.2019.2918560](https://doi.org/10.1109/ACCESS.2019.2918560).
- [26] H. Xiao, T. Chanwimalueang, and D. P. Mandic, "Multivariate multiscale cosine similarity entropy," in *Proc. IEEE Int. Conf. Acoust., Speech Signal Process. (ICASSP)*, May 2022, pp. 5997–6001, doi: [10.1109/ICASSP43922.2022.9747282](https://doi.org/10.1109/ICASSP43922.2022.9747282).
- [27] B. Deza and D. Deka, "An improved multiscale distribution entropy for analyzing complexity of real-world signals," *Chaos, Solitons Fractals*, vol. 158, May 2022, Art. no. 112101, doi: [10.1016/j.chaos.2022.112101](https://doi.org/10.1016/j.chaos.2022.112101).
- [28] H. Azami, M. Rostaghi, D. Abásolo, and J. Escudero, "Refined composite multiscale dispersion entropy and its application to biomedical signals," *IEEE Trans. Biomed. Eng.*, vol. 64, no. 12, pp. 2872–2879, Dec. 2017, doi: [10.1109/TBME.2017.2679136](https://doi.org/10.1109/TBME.2017.2679136).
- [29] H. B. Mann and D. R. Whitney, "On a test of whether one of two random variables is stochastically larger than the other," *Ann. Math. Statist.*, vol. 18, no. 1, pp. 50–60, Mar. 1947, doi: [10.1214/aoms/1177730491](https://doi.org/10.1214/aoms/1177730491).
- [30] C. E. Shannon, "A mathematical theory of communication," *Bell Syst. Tech. J.*, vol. 27, no. 3, pp. 379–423, Jul. 1948, doi: [10.1002/j.1538-7305.1948.tb01338.x](https://doi.org/10.1002/j.1538-7305.1948.tb01338.x).
- [31] E. Sejdić and L. A. Lipsitz, "Necessity of noise in physiology and medicine," *Comput. Methods Programs Biomed.*, vol. 111, no. 2, pp. 459–470, Aug. 2013, doi: [10.1016/j.cmpb.2013.03.014](https://doi.org/10.1016/j.cmpb.2013.03.014).
- [32] A. Borin, A. Humeau-Heurtier, L. V. Silva, and L. Murta, "Multiscale entropy analysis of short signals: The robustness of fuzzy entropy-based variants compared to full-length long signals," *Entropy*, vol. 23, no. 12, p. 1620, Dec. 2021, doi: [10.3390/e23121620](https://doi.org/10.3390/e23121620).
- [33] P. Castiglioni, G. Merati, G. Parati, and A. Faini, "Sample, fuzzy and distribution entropies of heart rate variability: What do they tell us on cardiovascular complexity?" *Entropy*, vol. 25, no. 2, p. 281, Feb. 2023, doi: [10.3390/e25020281](https://doi.org/10.3390/e25020281).
- [34] A. M. S. Borin, L. E. V. Silva, and L. O. Murta, "Modified multiscale fuzzy entropy: A robust method for short-term physiologic signals," *Chaos, Interdiscipl. J. Nonlinear Sci.*, vol. 30, no. 8, Aug. 2020, Art. no. 8, doi: [10.1063/5.0010330](https://doi.org/10.1063/5.0010330).

- [35] A. L. Goldberger, L. A. N. Amaral, L. Glass, J. M. Hausdorff, P. C. Ivanov, R. G. Mark, J. E. Mietus, G. B. Moody, C.-K. Peng, and H. E. Stanley, "PhysioBank, PhysioToolkit, and PhysioNet: Components of a new research resource for complex physiologic signals," *Circulation*, vol. 101, no. 23, pp. 215–220, Jun. 2000, doi: [10.1161/01.cir.101.23.e215](https://doi.org/10.1161/01.cir.101.23.e215).
- [36] D. S. Baim, W. S. Colucci, E. S. Monrad, H. S. Smith, R. F. Wright, A. Lanoue, D. F. Gauthier, B. J. Ransil, W. Grossman, and E. Braunwald, "Survival of patients with severe congestive heart failure treated with oral milrinone," *J. Amer. College Cardiol.*, vol. 7, no. 3, pp. 661–670, Mar. 1986, doi: [10.1016/s0735-1097\(86\)80478-8](https://doi.org/10.1016/s0735-1097(86)80478-8).
- [37] G. Moody, "A new method for detecting atrial fibrillation using R–R intervals," *Proc. Comput. Cardiol.*, no. 10, pp. 227–230, Jan. 1983.
- [38] N. Iyengar, C. K. Peng, R. Morin, A. L. Goldberger, and L. A. Lipsitz, "Age-related alterations in the fractal scaling of cardiac interbeat interval dynamics," *Amer. J. Physiol.-Regulatory, Integrative Comparative Physiol.*, vol. 271, no. 4, pp. 1078–1084, Oct. 1996, doi: [10.1152/ajpregu.1996.271.4.r1078](https://doi.org/10.1152/ajpregu.1996.271.4.r1078).
- [39] J. C. Moses, S. Adibi, M. Angelova, and S. M. S. Islam, "Time-domain heart rate variability features for automatic congestive heart failure prediction," *ESC Heart Failure*, vol. 11, no. 1, pp. 378–389, Feb. 2024, doi: [10.1002/ehf2.14593](https://doi.org/10.1002/ehf2.14593).
- [40] L. Zou, Z. Huang, X. Yu, J. Zheng, A. Liu, and M. Lei, "Automatic detection of congestive heart failure based on multiscale residual UNet++: From centralized learning to federated learning," *IEEE Trans. Instrum. Meas.*, vol. 72, pp. 1–13, 2023, doi: [10.1109/TIM.2022.3227955](https://doi.org/10.1109/TIM.2022.3227955).
- [41] Y. Li and Y. Xia, "Atrial fibrillation detection with signal decomposition and dilated residual neural network," *Physiol. Meas.*, vol. 44, no. 10, Oct. 2023, Art. no. 105001, doi: [10.1088/1361-6579/acfa61](https://doi.org/10.1088/1361-6579/acfa61).
- [42] H. C. Fogedby, "On the phase space approach to complexity," *J. Stat. Phys.*, vol. 69, nos. 1–2, pp. 411–425, Oct. 1992, doi: [10.1007/bf01053799](https://doi.org/10.1007/bf01053799).
- [43] J. Pan and W. J. Tompkins, "A real-time QRS detection algorithm," *IEEE Trans. Biomed. Eng.*, vol. BME-32, no. 3, pp. 230–236, Mar. 1985, doi: [10.1109/TBME.1985.325532](https://doi.org/10.1109/TBME.1985.325532).
- [44] Q. Xiao, K. Lee, S. A. Mokhtar, I. Ismail, A. L. B. M. Pauzi, Q. Zhang, and P. Y. Lim, "Deep learning-based ECG arrhythmia classification: A systematic review," *Appl. Sci.*, vol. 13, no. 8, p. 4964, Apr. 2023, doi: [10.3390/app13084964](https://doi.org/10.3390/app13084964).



CHAE-MIN KIM received the B.S. degree from the Division of Robotics, Kwangwoon University, Seoul, South Korea, in 2023, where he is currently pursuing the integrated M.S. and Ph.D. degrees with the Department of Electronics and Communications Engineering.



YOUNG-SEOK CHOI (Member, IEEE) received the B.S. degree in electronic and electrical engineering from Hanyang University, Seoul, South Korea, in 2000, and the Ph.D. degree in electrical and computer engineering from Pohang University of Science and Technology (POSTECH), Pohang, South Korea, in 2007. From 2007 to 2010, he was a Postdoctoral Fellow with the Department of Biomedical Engineering, The Johns Hopkins University School of Medicine, Baltimore, MD, USA. From 2010 to 2012, he was a Senior Researcher with the Electronics and Telecommunications Research Institute, Daejeon, South Korea. From 2012 to 2016, he was an Assistant Professor with the Department of Electronic Engineering, Gangneung–Wonju National University, Gangneung, South Korea. In 2016, he joined as a Faculty Member with Kwangwoon University, Seoul, where he is currently a Professor of electronics and communications engineering. His current research interests include computational neural engineering, neuromorphic engineering, brain–computer interface, affective computing, and human-centered intelligence.

• • •